The Supporting Information for

Rotaxane formation by an allosteric pseudomacrocyclic anion receptor utilising kinetically labile copper(I) coordination properties

Taeko Aizawa, Shigehisa Akine, Toshiyuki Saiki, Takashi Nakamura and Tatsuya Nabeshima*

Faculty of Pure and Applied Sciences

and Tsukuba Research Center for Energy Materials Science (TREMS),

University of Tsukuba, 1-1-1 Tennodai, Tsukuba, Ibaraki 305-8571, Japan

*Corresponding Author. E-mail: nabesima@chem.tsukuba.ac.jp

Contents

Materials and methods

Unless otherwise noted, solvents and reagents were purchased from TCI Co., Ltd., Wako Pure Chemical Co., Ltd., Kanto Chemical Co., Inc., Nacalai Tesque, Inc. or Sigma-Aldrich Co., and used without further purification. THF was distilled from sodium benzophenone ketyl prior to use.

Measurements were performed at 298 K unless otherwise noted. NMR spectra were recorded on Bruker AC300, ARX400 or AV600 spectrometers. Tetramethylsilane was used as an internal standard (δ 0.00 ppm) for ^{1}H and ^{13}C NMR measurements.

ESI-TOF mass data were recorded on an Applied Biosystems QStar Pulsar i spectrometer. UV-vis spectra were recorded on a JASCO V-570 spectrometer. IR spectra were recorded on a JASCO FT/IR-480Plus spectrometer. Elemental analyses were performed at Chemical Analysis Center, University of Tsukuba. We appreciate Mr. Ikuo Iida for the elemental analysis measurements.

The structural calculations of the complexes were performed on a Spartan'18 software (Wavefunction Inc., *ver* 1.4.1 (2019)). The initial structures of $(3,5\text{-di-}t\text{BuC}_6\text{H}_3\text{O})_2\text{P(O)O}^-$ ⊂ $[\mathbf{1}\cdot\text{Cu}]^+$ were optimized by molecular mechanics calculations (MMFF), then the obtained structures were optimized by semi-empirical calculations (PM6).

Synthesis of ligand 1 and complex [1·Cu]PF_6

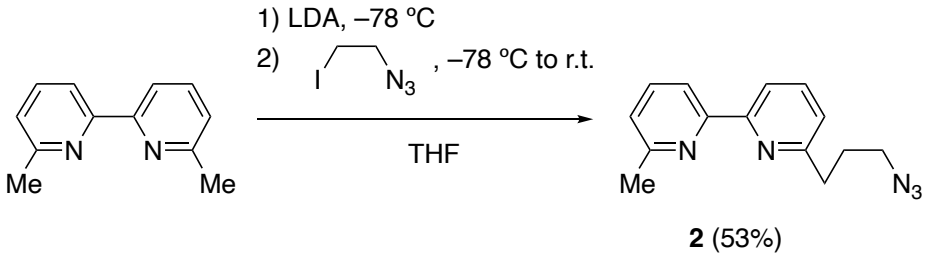

Scheme S1. Synthesis of **2**

Synthesis of **2**

6,6′-dimethyl-2,2′-bipyridine (502 mg, 2.72 mmol) was placed in a three-necked round-bottom flask, and dried in vacuo at room temperature for 2 h. Dry THF (40 mL) was added to the flask under an Ar atmosphere. The solution was cooled to –78 °C, and 1.50 mL of dry THF solution of LDA (2.0 M, 3.00 mmol) was added dropwise, and then stirred for 1 h at the same temperature. Next, 20 mL of dry THF solution of 1-azide-2-iodoethane[S1] (1.00 g, 5.08 mmol) was added dropwise. The mixture was gradually warmed to room temperature with stirring for 6 h. The mixture was cooled in an ice bath, and 10 mL of aqueous solution of NaOH (0.5 M) was added. The mixture was extracted with Et_2O (20 mL × 4), and the combined organic layer was dried over K_2CO_3, filtered, and concentrated in vacuo. The obtained yellow oil was purified by column chromatography (silica gel, eluent: $CHCl_3$/AcOEt = 10/1) to obtain **2** (242 mg, 0.955 mmol, 35%) as a pale yellow oil.

2: Pale yellow oil; ^{1}H NMR (300 MHz, $CDCl_3$) δ 2.15 (quint, J = 7.2 Hz, 2H), 2.63 (s, 3H), 2.95 (t, J = 7.2 Hz, 2H), 3.39 (t, J = 7.2 Hz, 2H), 7.15 (d, J = 7.2 Hz, 1H), 7.17 (d, J = 7.2 Hz, 1H), 7.70 (t, J = 7.2 Hz, 1H), 7.72 (t, J = 7.2 Hz, 1H), 8.22 (d, J = 7.2 Hz, 1H), 8.24 (d, J = 7.2 Hz, 1H).

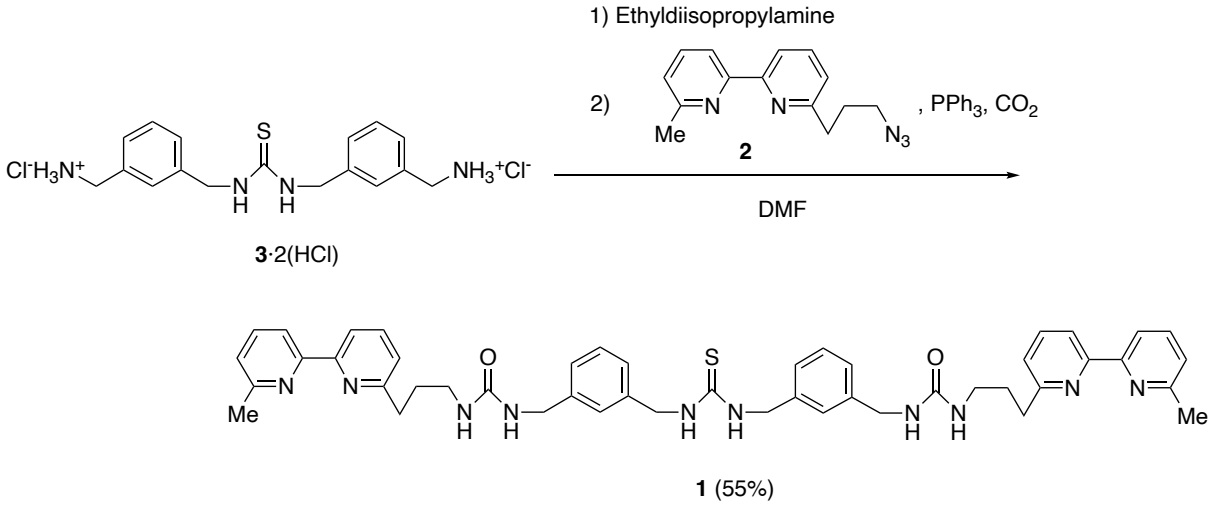

Scheme S2. Synthesis of **1**

Synthesis of **1**

3·2(HCl) (155 mg, 0.398 mmol), a hydrochloride salt of diamine **3**[S2], was placed in 30 mL a two-necked round-bottom flask, and the atmosphere was replaced with argon. Dry DMF (14 mL) was added to the flask, and diisopropylethylamine (1.54 g, 2.1 mL, 11.94 mmol) was added dropwise to the resulting solution with stirring. The solution was stirred for 2 h. This solution was added to azide **2** (242 mg, 0.955 mmol), which was dried in vacuo at room temperature for 30 min and placed under an argon atmosphere prior to use. PPh_3 (476 mg, 1.81 mmol) was added to the flask, and the mixture was stirred at room temperature for 48 h with CO_2 bubbling. The solvent was removed in vacuo, and the obtained yellow oil was purified by column chromatography (silica gel (pretreated with $CHCl_3$/MeOH = 7/3), eluent: $CHCl_3$/MeOH = 100/1→10/1). To the obtained residue was added chloroform (100 mL), and washed with H_2O (100 mL × 2), dried over $MgSO_4$, filtered, and dried in vacuo. CH_2Cl_2 and CH_3OH were added to the obtained residue, and CH_2Cl_2 was removed under reduced pressure. Colorless solid appeared in the methanol-rich solution, which was collected by filtration to obtain **1** (180 mg, 0.220 mmol, 55%).

1: Colorless solid, mp 169–171 ºC; ^{1}H NMR (600 MHz, $CDCl_3$/DMSO-d_6 = 1/1): δ 1.93 (m, 4H), 2.58 (s, 6H), 2.84 (m, 4H), 3.18 (m, 4H), 4.25 (d, J = 4.7 Hz, 4H), 4.70 (br, 4H), 5.97 (m, 2H), 6.27 (br, 2H), 7.15–7.26 (12H), 7.71–7.78 (6H), 8.20–8.22 (4H); ^{13}C NMR (150 MHz, $CDCl_3$/DMSO-d_6 = 1/1) δ 24.35, 30.01, 35.07, 39.10, 43.20, 117.64, 117.83, 122.58, 122.99, 125.72, 125.80, 126.18, 128.20, 136.87, 136.93, 139.01, 140.82, 155.04, 155.12, 157.23, 158.34, 160.60; FT-IR (KBr) 3315, 3061, 2923, 2865, 1636, 1622, 1573, 1440, 1374, 1351, 1336, 1255, 1152, 1083, 991, 959 cm^{-1}; Anal. Calcd for $C_{47}H_{52}N_{10}O_2S$: C, 68.75; H, 6.38; N, 17.06. Found: C, 68.31; H, 6.37; N, 17.46; ESI-MS observed m/z 411.21 ($[M+2H]^{2+}$), 821.38 ($[M+H]^+$).

Synthesis of complex [**1**·Cu]PF_6

The ligand **1** (123.2 mg, 0.15 mmol) was dissolved in a $CHCl_3/CH_3OH$ = 10/1 mixed solvent (20 mL). A CH_3CN solution (30 mL) of $[Cu(CH_3CN)_4]PF_6$ (55.91 mg, 0.15 mmol) was added to the solution, and the solvent was removed in vacuo. The residue was dissolved in a $CHCl_3/CH_3CN$ = 10/1 mixed solvent (5 mL), and then Et_2O (30 mL) was added. The precipitate was collected by filtration to obtain [**1**·Cu]PF_6 (143.9 mg, 0.139 mmol, 93%) as a pale orange solid.

[**1**·Cu]PF_6: pale orange solid; ^{1}H NMR (400 MHz, $CDCl_3/CD_3CN$/DMSO-d_6 = 15/1/4) δ 1.56 (m, 4H), 2.18 (s, 6H), 2.54–2.67 (6H), 2.83 (m, 2H), 4.11 (br, 4H), 4.71 (br, 4H), 5.63 (br, 2H), 6.40 (m, 2H), 7.05–7.28 (8H), 7.47 (d, J = 7.6 Hz, 2H), 7.53 (d, J = 8.0 Hz, 2H), 7.98–8.04 (4H), 8.22–8.27 (m, 4H); ^{13}C NMR (150 MHz, $CDCl_3/CD_3CN$/DMSO-d_6 = 15/1/4) δ 24.85, 29.29, 36.69, 39.10, 43.57, 119.64, 120.07, 125.30, 125.94, 126.19, 128.40, 138.43, 138.54, 151.62, 151.69, 156.95, 158.54, 160.31; FT-IR (KBr) 3435, 2925, 1647, 1597, 1562, 1464, 1440, 1376, 1356, 1335, 1257, 1173, 1084, 961, 847 cm^{-1}; Anal. Calcd for $C_{47}H_{52}CuF_6N_{10}O_2PS$: C, 54.83; H, 5.09; N, 13.60. Found: C, 54.61; H, 5.17; N, 13.40; ESI-MS (M = **1**·Cu^+) observed m/z 883.33 ($[M]^+$).

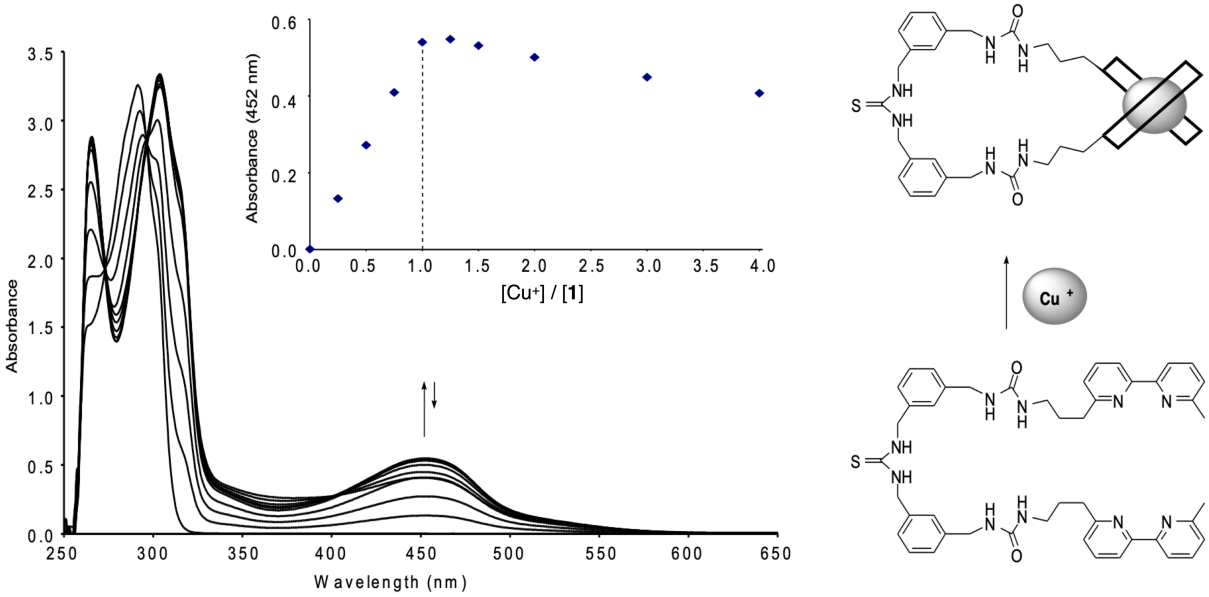

Figure S1. A titration experiment of **1** and $[Cu(CH_3CN)_4]PF_6$ (UV-vis absorption, DMF/CH_3CN = 1/1, [**1**] = 100 μM, l = 1.0 cm).

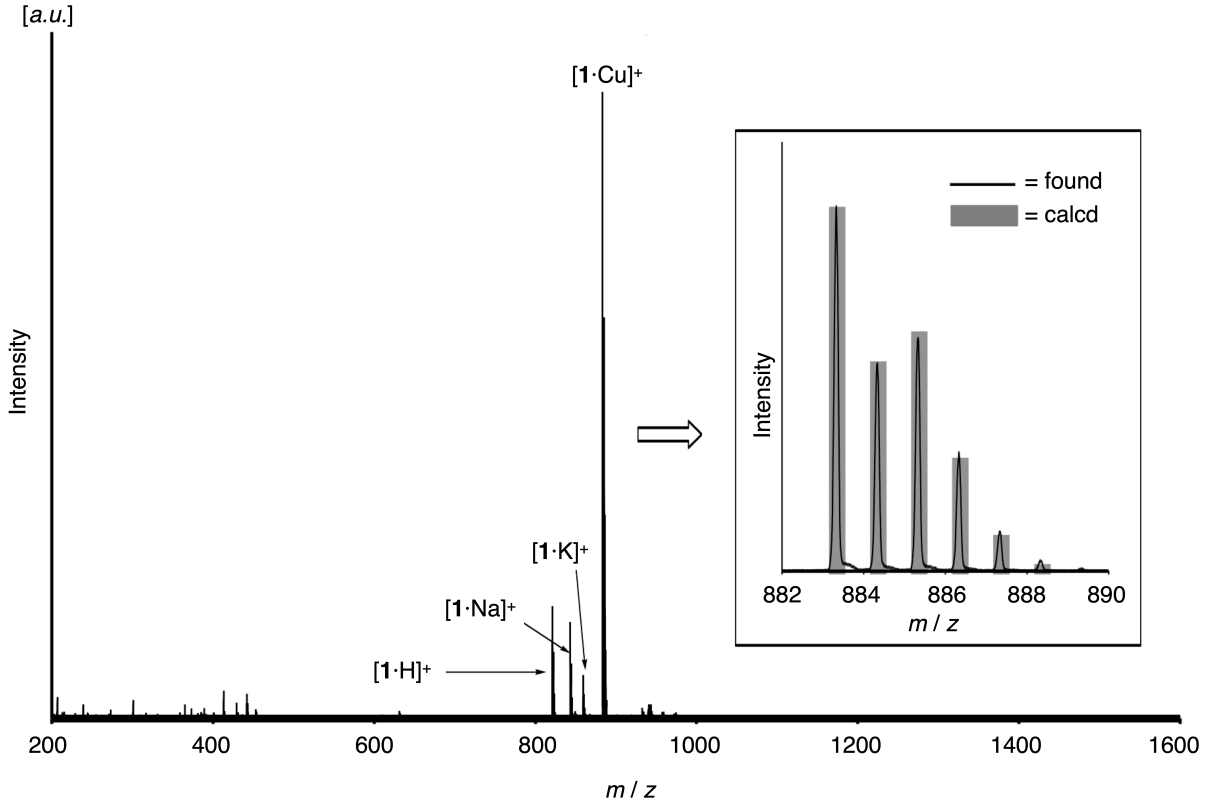

Figure S2. ESI TOF mass spectrum of [**1**·Cu]PF_6.

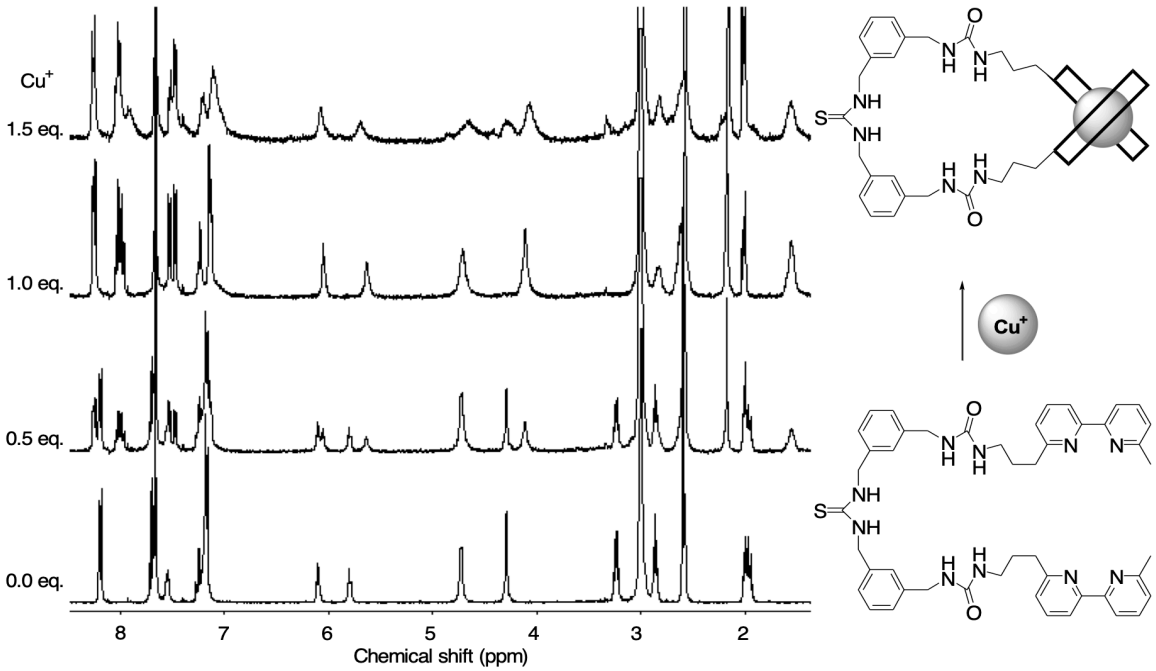

Figure S3. A titration experiment of **1** and [Cu(CH_3CN)$_4$]PF_6 (^{1}H NMR, $CDCl_3$/CD_3CN/DMSO-d_6 = 15/1/4, 400 MHz, [**1**] = 2.0 mM).

Anion titration experiments of 1 and $[1\cdot Cu]^+$

A representative procedure: ^{1}H NMR titration experiment of nBu$_4$NCl and ligand **1**

The ligand **1** (8.21 mg, 10.0 μmol) was dissolved in $CHCl_3/CH_3OH$ = 10/1, and a 2.00 mM solution of **1** was prepared in a 5 mL volumetric flask. nBu$_4$NCl (27.79 mg, 100.0 μmol) was dissolved in $CHCl_3$, and a 10.00 mM solution of nBu$_4$NCl was prepared in a 10 mL volumetric flask. 500 μL of the solution of **1** (1.00 μmol) was added to 9 NMR tubes. The solution of nBu$_4$NCl was added to each NMR tube with a ratio of $[Cl^-]/[\mathbf{1}]$ = 0, 0.25, 0.50, 0.75, 1.0, 1.25, 1.5, 2.0, 3.0, respectively. The solvents were removed under reduced pressure, and the samples were dried in vacuo for 5 h. DMSO-d_6 (100 μL) were added to each NMR tube to dissolve the solid. Then 400 μL of $CDCl_3/CD_3CN$ = 15/1 were added to prepare the samples ([**1**] = 2.00 mM), and ^{1}H NMR measurements were performed. The binding constant between **1** and Cl^- was evaluated from the least square fitting of the chemical shift changes of signals *h* and *i* (see Fig. S4 for the assignment).

A representative procedure: ^{1}H NMR titration experiment of nBu$_4$NCl and complex [**1**·Cu]PF$_6$

The complex [**1**·Cu]PF$_6$ (10.3 mg, 10.0 μmol) was dissolved in $CHCl_3/CH_3CN$ = 1/1, and a 2.00 mM solution of **1** was prepared in a 5 mL volumetric flask. nBu$_4$NCl (27.79 mg, 100.0 μmol) was dissolved in $CHCl_3$, and a 10.00 mM solution of nBu$_4$NCl was prepared in a 10 mL volumetric flask. 500 μL of the solution of [**1**·Cu]PF$_6$ (1.00 μmol) was added to 9 NMR tubes. The solution of nBu$_4$NCl was added to each NMR tube with a ratio of $[Cl^-]/[\mathbf{1}\cdot Cu]$ = 0, 0.25, 0.50, 0.75, 1.0, 1.25, 1.5, 2.0, 3.0, respectively. The solvents were removed under reduced pressure, and the samples were dried in vacuo for 5 h. DMSO-d_6 (100 μL) were added to each NMR tube to dissolve the solid. Then 400 μL of $CDCl_3/CD_3CN$ = 15/1 were added to prepare the samples ([**1**·Cu] = 2.00 mM), and ^{1}H NMR measurements were performed. The binding constant between $[\mathbf{1}\cdot Cu]^+$ and Cl^- was evaluated from the least square fitting of the chemical shift changes of signals *h* and *i* (see Fig. S16 for the assignment).

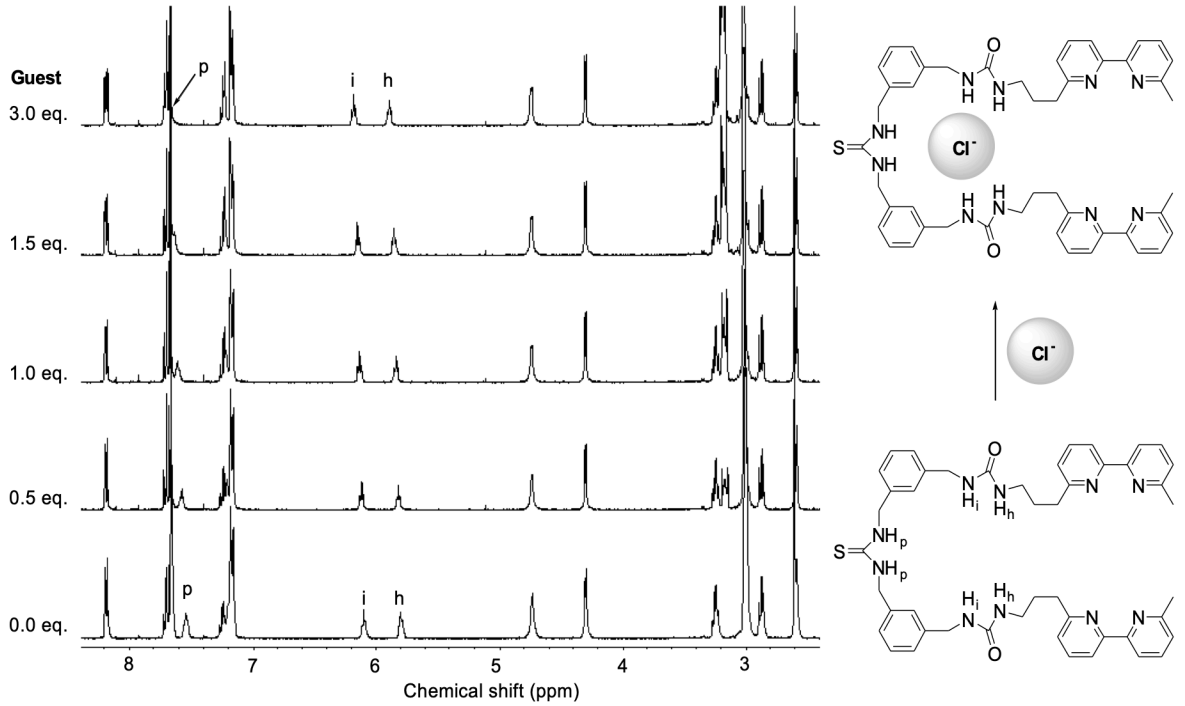

Figure S4. A titration experiment of **1** and nBu$_4$NCl (^{1}H NMR, $CDCl_3/CD_3CN$/DMSO-d_6 = 15/1/4, 400 MHz, [**1**] = 2.0 mM).

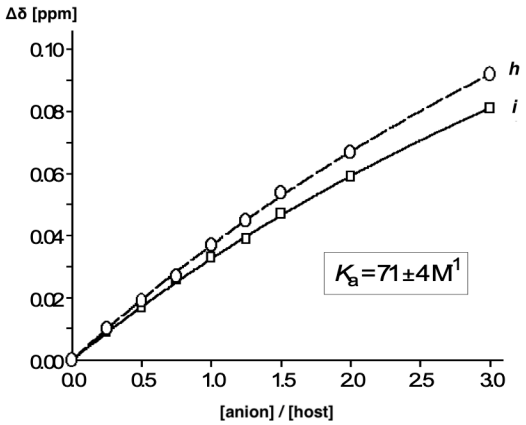

Figure S5. A least squares fitting to determine the binding constant K_a of Cl^- and **1** (data of NMR signals of urea ^{1}H(*h* and *i*)).

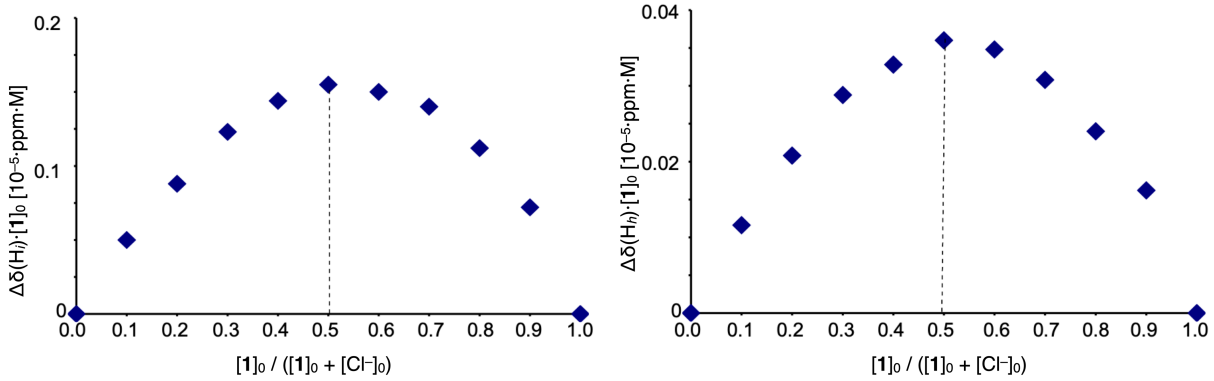

Figure S6. Job plots to determine the binding stoichiometry of Cl^- and **1** (^{1}H NMR, $CDCl_3/CD_3CN$/DMSO-d_6 = 15/1/4, 400 MHz, $[\mathbf{1}]_0 + [Cl^-]_0$ = 4.0 mM, data of NMR signals of urea ^{1}H(*h* and *i*)).

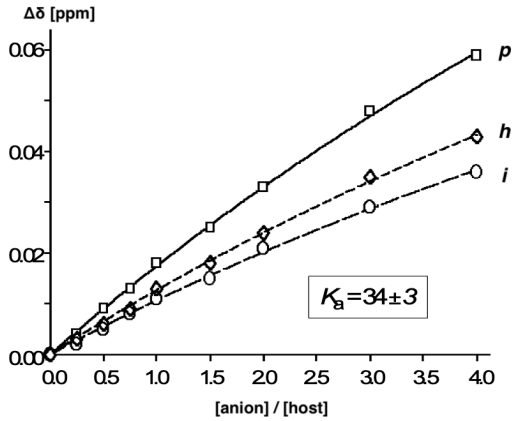

Figure S7. A least squares fitting to determine the binding constant K_a of Br^- and **1** (data of NMR signals of urea ^{1}H(*h* and *i*) and thiourea ^{1}H(*p*)).

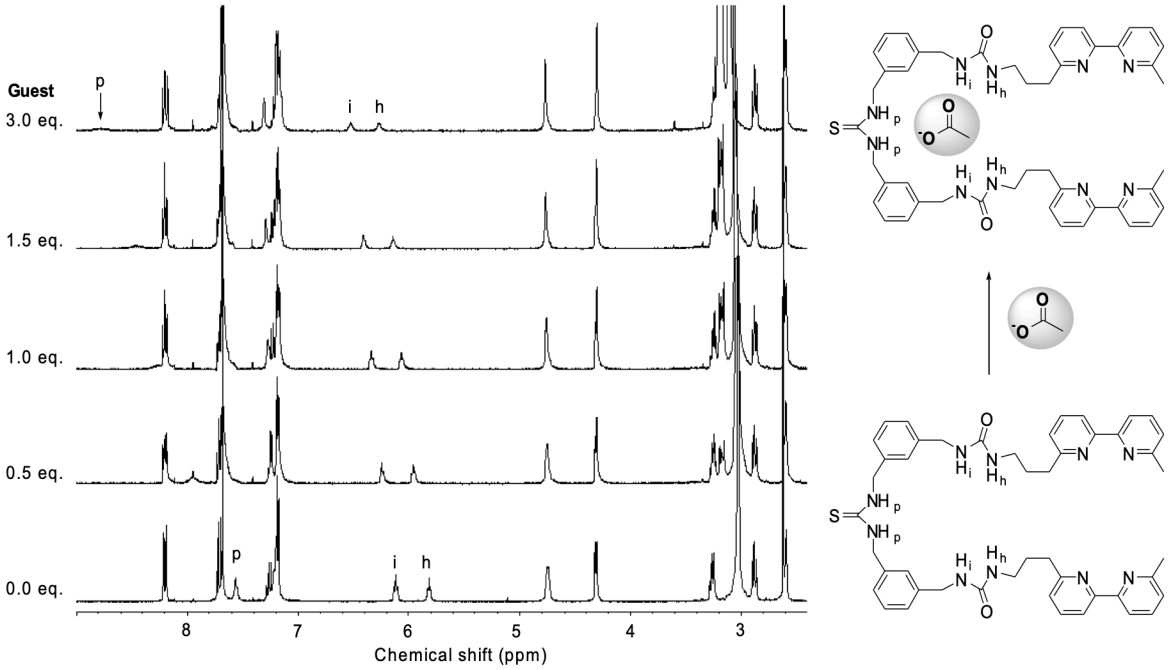

Figure S8. A titration experiment of **1** and nBu$_4$NOAc (^{1}H NMR, $CDCl_3$/CD_3CN/DMSO-d_6 = 15/1/4, 400 MHz, [**1**] = 2.0 mM).

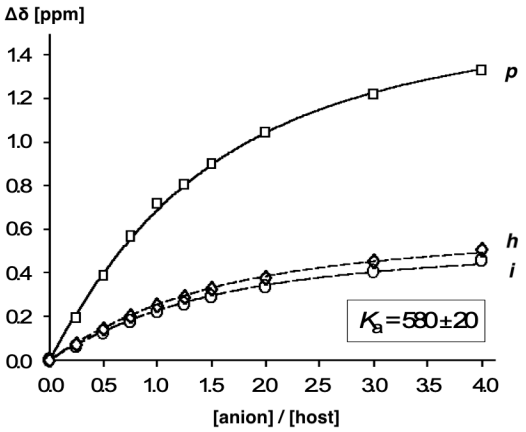

Figure S9. A least squares fitting to determine the binding constant K_a of AcO^- and **1** (data of NMR signals of urea ^{1}H(*h* and *i*) and thiourea ^{1}H(*p*)).

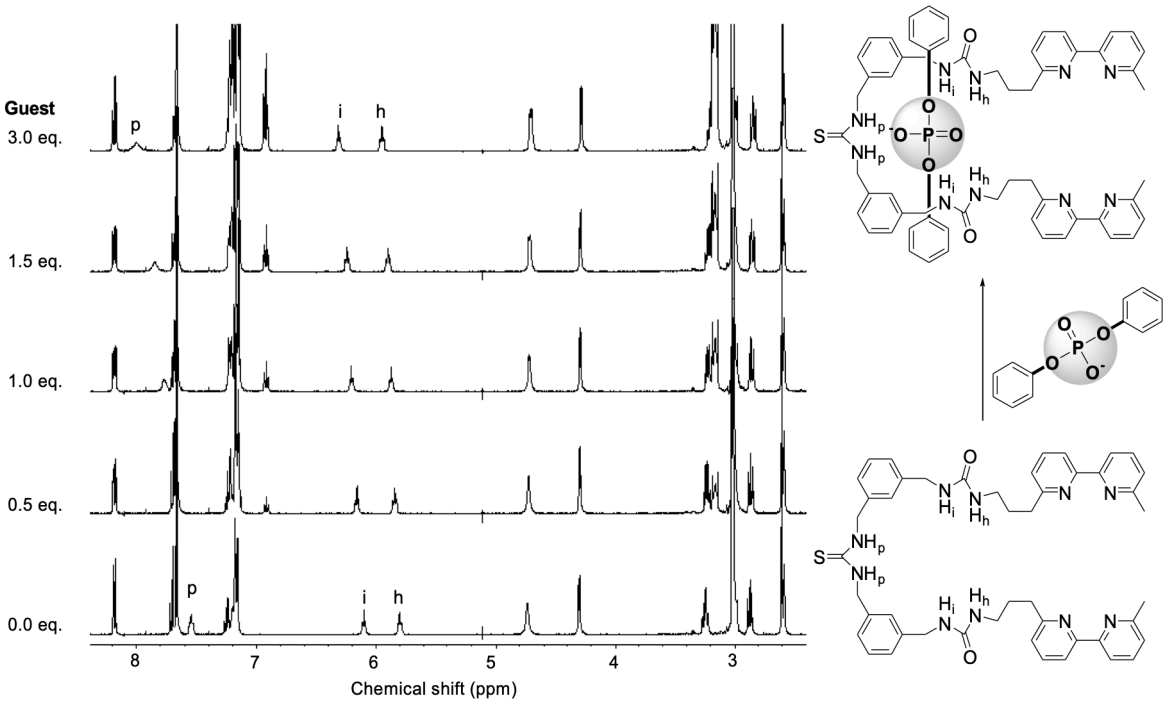

Figure S10. A titration experiment of **1** and nBu$_4$N[(PhO)$_2$P(O)O] (^{1}H NMR, $CDCl_3$/CD_3CN/DMSO-d_6 = 15/1/4, 400 MHz, [**1**] = 2.0 mM).

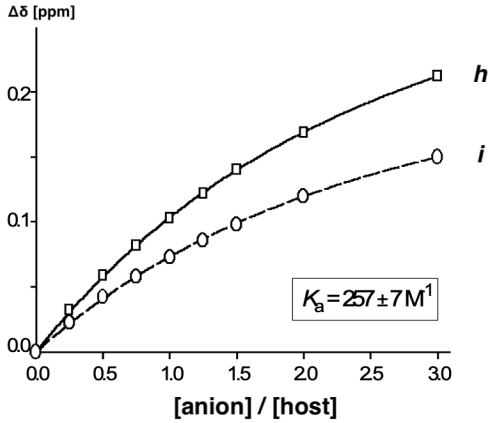

Figure S11. A least squares fitting to determine the binding constant K_a of (PhO)$_2$P(O)O$^-$ and **1** (data of NMR signals of urea ^{1}H(*h* and *i*)).

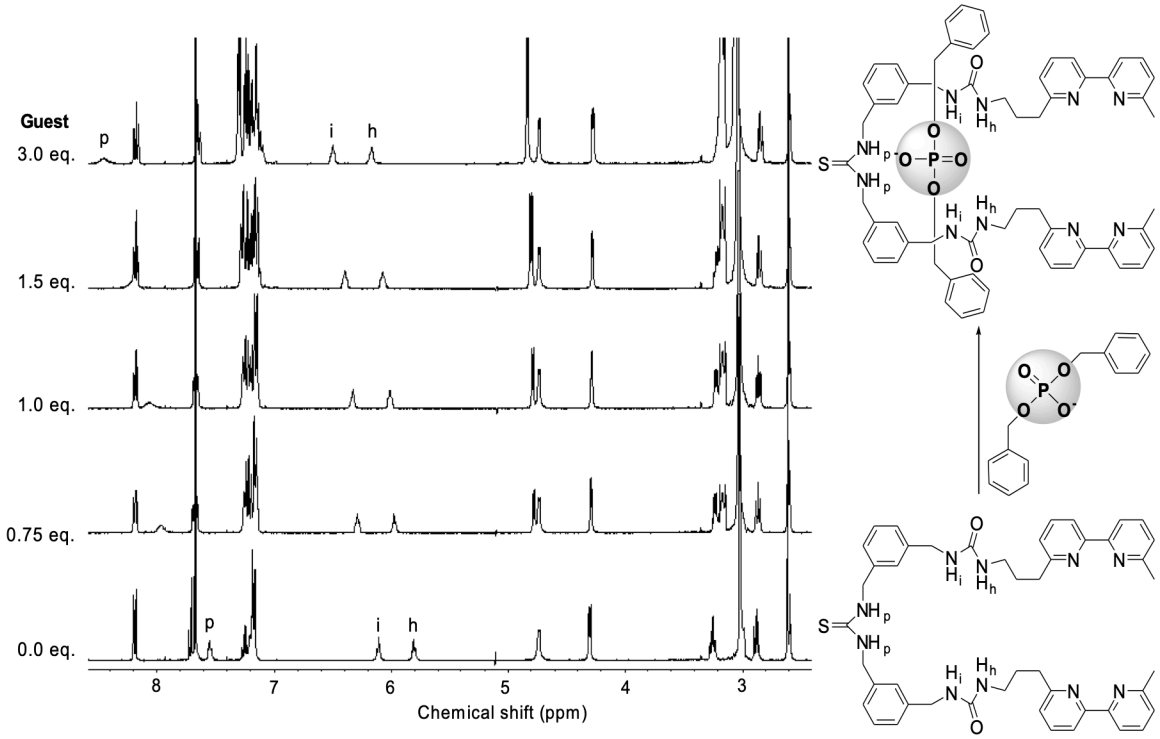

Figure S12. A titration experiment of **1** and nBu$_4$N[(BnO)$_2$P(O)O] (^{1}H NMR, $CDCl_3$/CD_3CN/DMSO-d_6 = 15/1/4, 400 MHz, [**1**] = 2.0 mM).

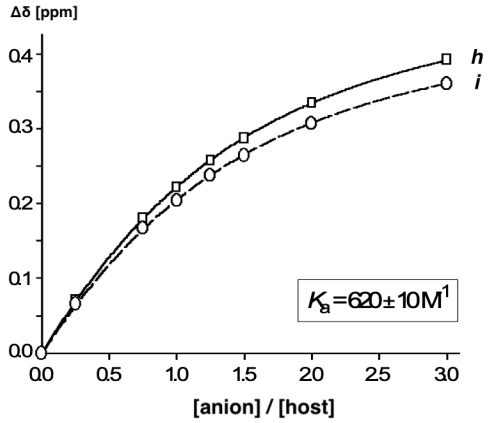

Figure S13. A least squares fitting to determine the binding constant K_a of (BnO)$_2$P(O)O$^-$ and **1** (data of NMR signals of urea ^{1}H(*h* and *i*)).

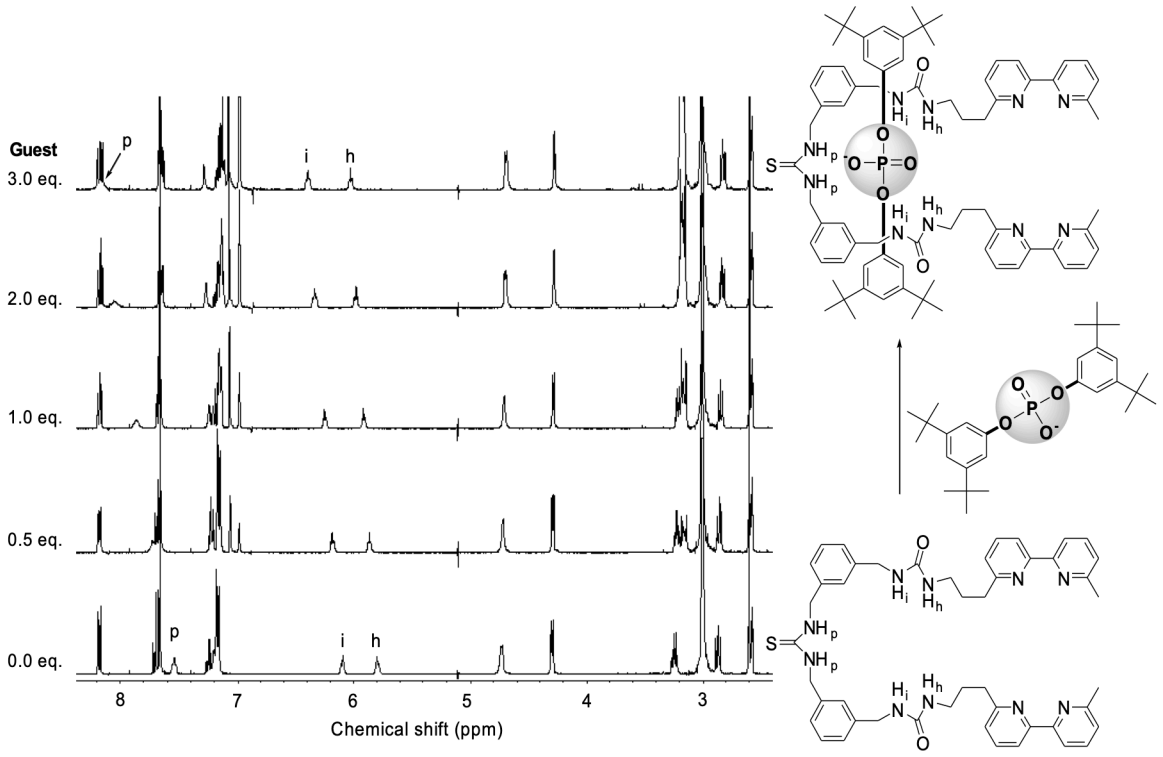

Figure S14. A titration experiment of **1** and nBu$_4$N[(3,5-di-tBuC$_6$H$_3$O)$_2$P(O)O] (^{1}H NMR, CDCl$_3$/CD$_3$CN/DMSO-d_6 = 15/1/4, 400 MHz, [**1**] = 2.0 mM).

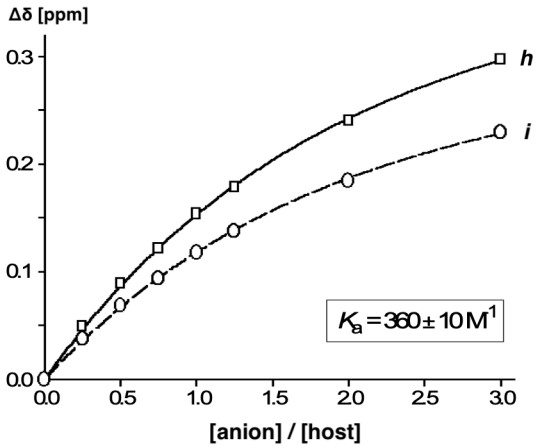

Figure S15. A least squares fitting to determine the binding constant K_a of (3,5-di-tBuC$_6$H$_3$O)$_2$P(O)O$^-$ and **1** (data of NMR signals of urea ^{1}H(*h* and *i*)).

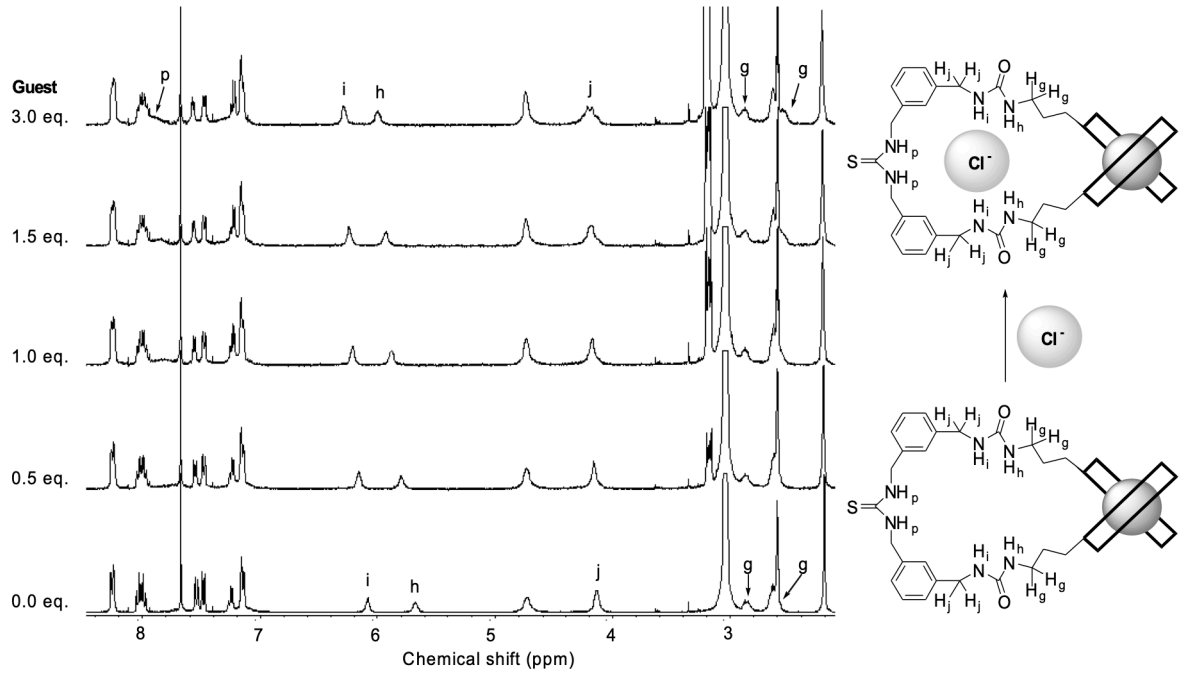

Figure S16. A titration experiment of [**1**·Cu]PF_6 and nBu$_4$NCl (^{1}H NMR, $CDCl_3$/CD_3CN/DMSO-d_6 = 15/1/4, 400 MHz, [**1**·Cu] = 2.0 mM).

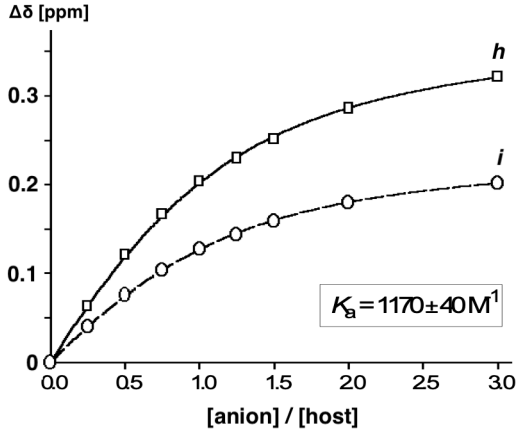

Figure S17. A least squares fitting to determine the binding constant K_a of Cl^- and [**1**·Cu]$^+$ (data of NMR signals of urea ^{1}H(*h* and *i*)).

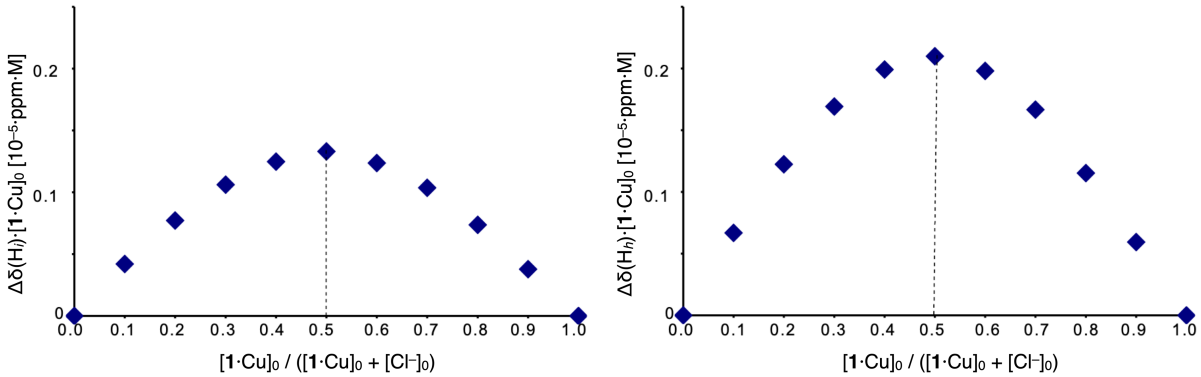

Figure S18. Job plots to determine the binding stoichiometry of Cl^- and [**1**·Cu]$^+$ (^{1}H NMR, $CDCl_3$/CD_3CN/DMSO-d_6 = 15/1/4, 400 MHz, [**1**·Cu]$_0$ + [Cl^-]$_0$ = 4.0 mM, data of NMR signals of urea ^{1}H(*h* and *i*)).

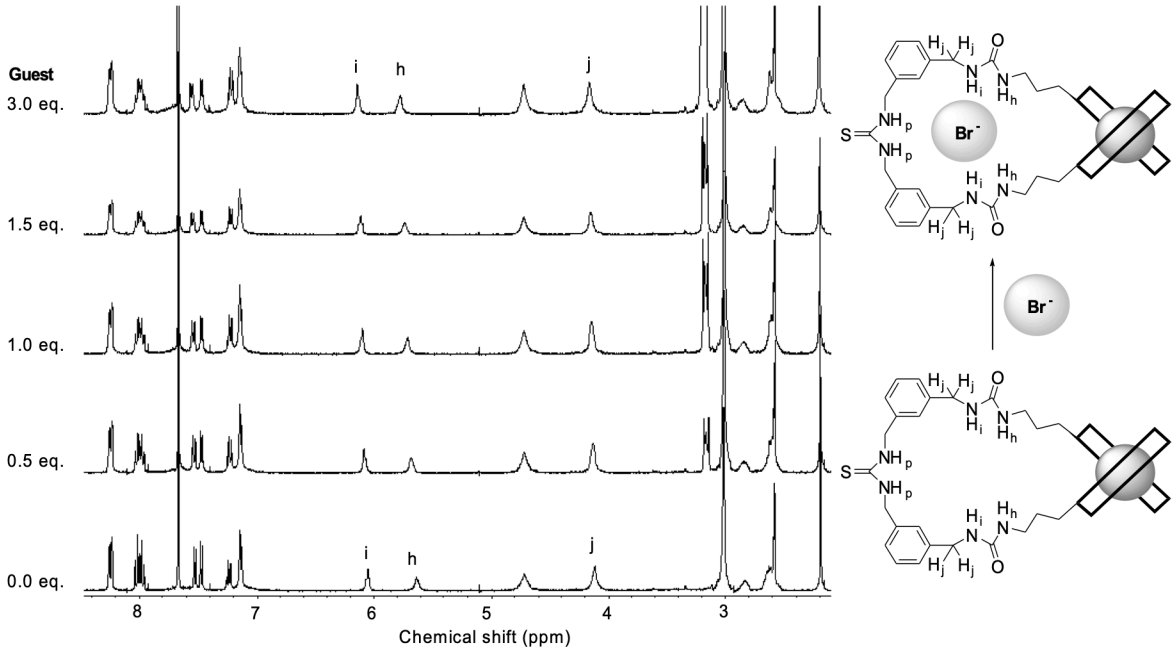

Figure S19. A titration experiment of [**1**·Cu]PF_6 and nBu$_4$NBr (^{1}H NMR, $CDCl_3$/CD_3CN/DMSO-d_6 = 15/1/4, 400 MHz, [**1**·Cu] = 2.0 mM).

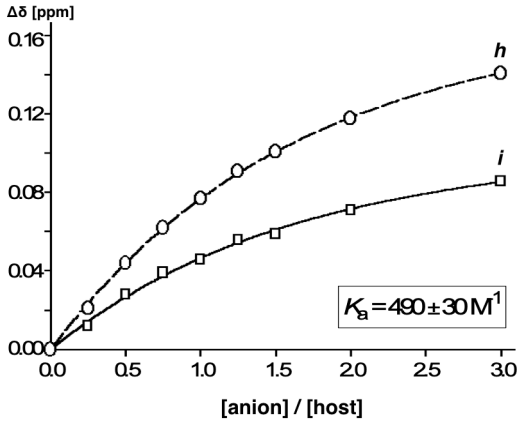

Figure S20. A least squares fitting to determine the binding constant K_a of Br^- and [**1**·Cu]$^+$ (data of NMR signals of urea ^{1}H(*h* and *i*)).

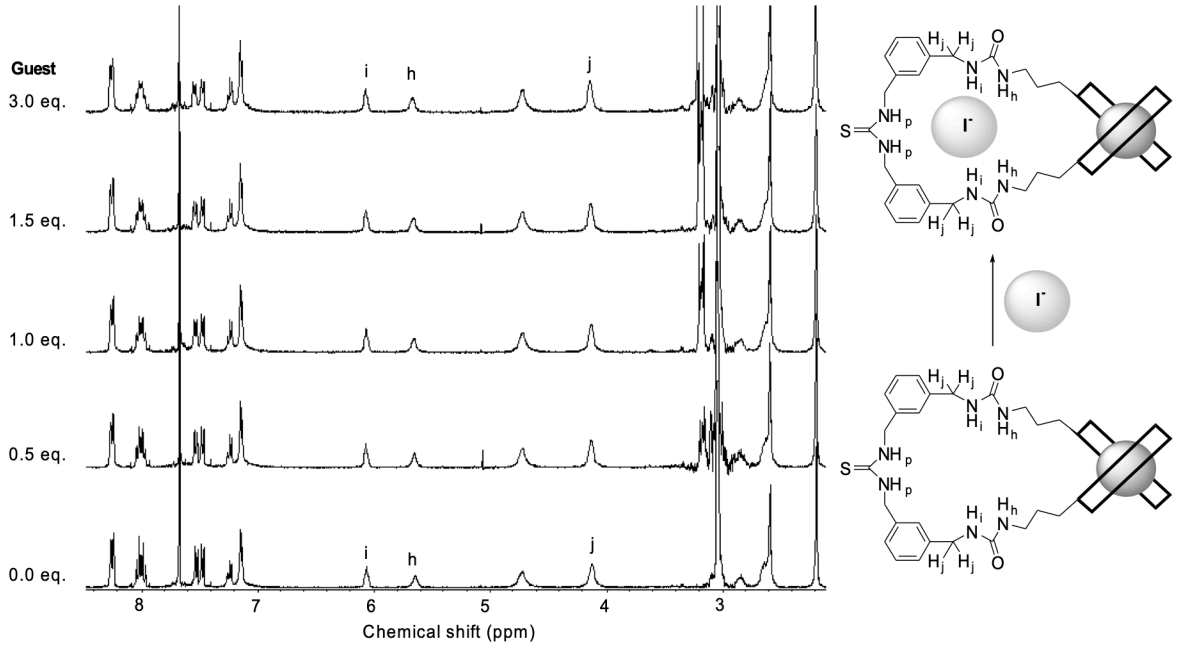

Figure S21. A titration experiment of [**1**·Cu]PF_6 and $n$$Bu_4NI$ (^{1}H NMR, $CDCl_3$/CD_3CN/DMSO-d_6 = 15/1/4, 400 MHz, [**1**·Cu] = 2.0 mM).

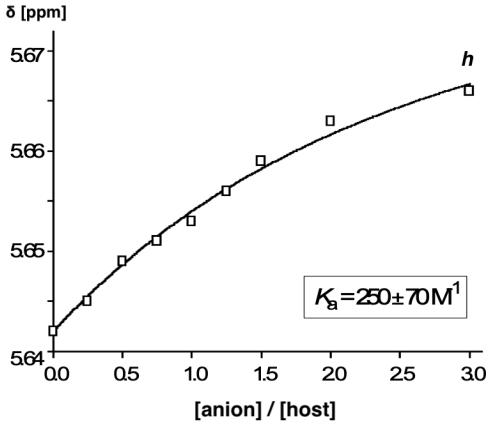

Figure S22. A least squares fitting to determine the binding constant K_a of I^- and [**1**·Cu]$^+$ (data of NMR signals of urea ^{1}H(h)).

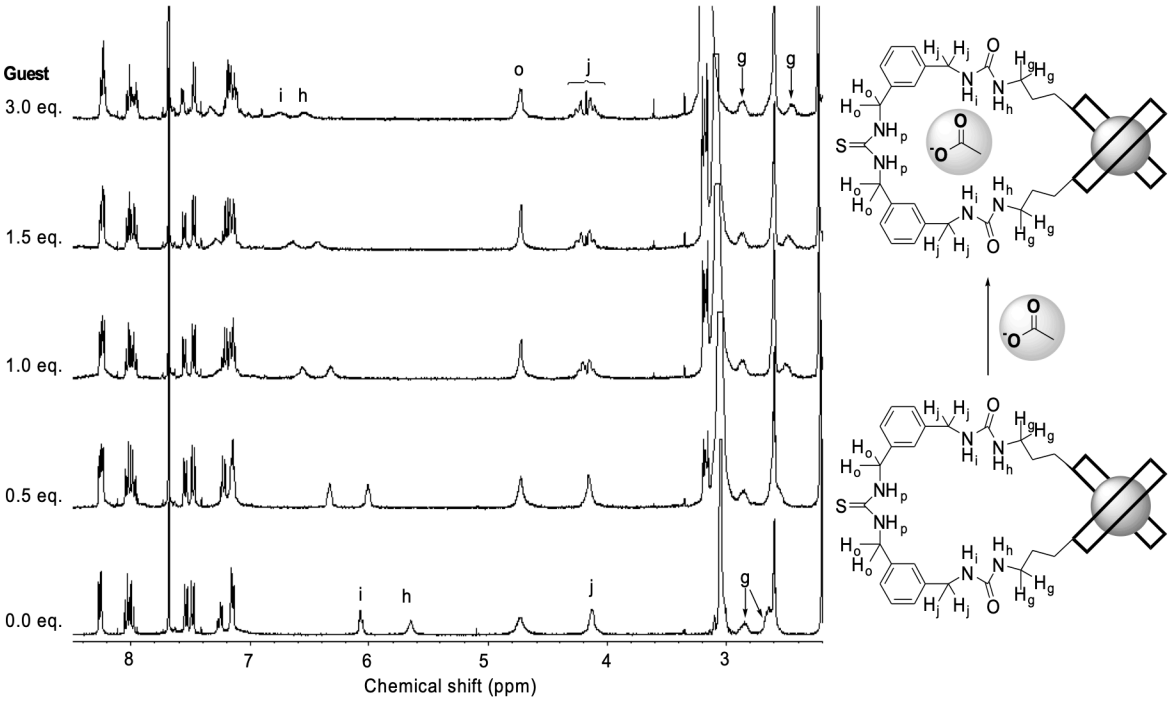

Figure S23. A titration experiment of [**1**·Cu]PF_6 and nBu$_4$NOAc (^{1}H NMR, $CDCl_3$/CD_3CN/DMSO-d_6 = 15/1/4, 400 MHz, [**1**·Cu] = 2.0 mM).

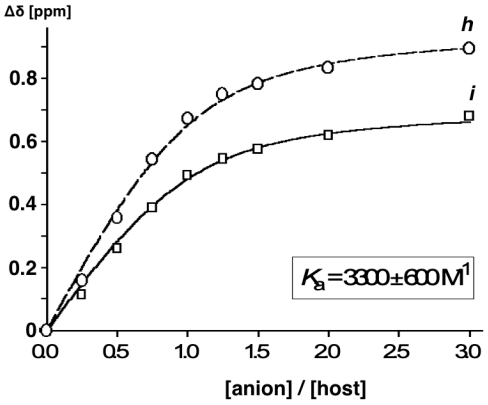

Figure S24. A least squares fitting to determine the binding constant K_a of AcO^- and [**1**·Cu]$^+$ (data of NMR signals of urea ^{1}H(*h* and *i*)).

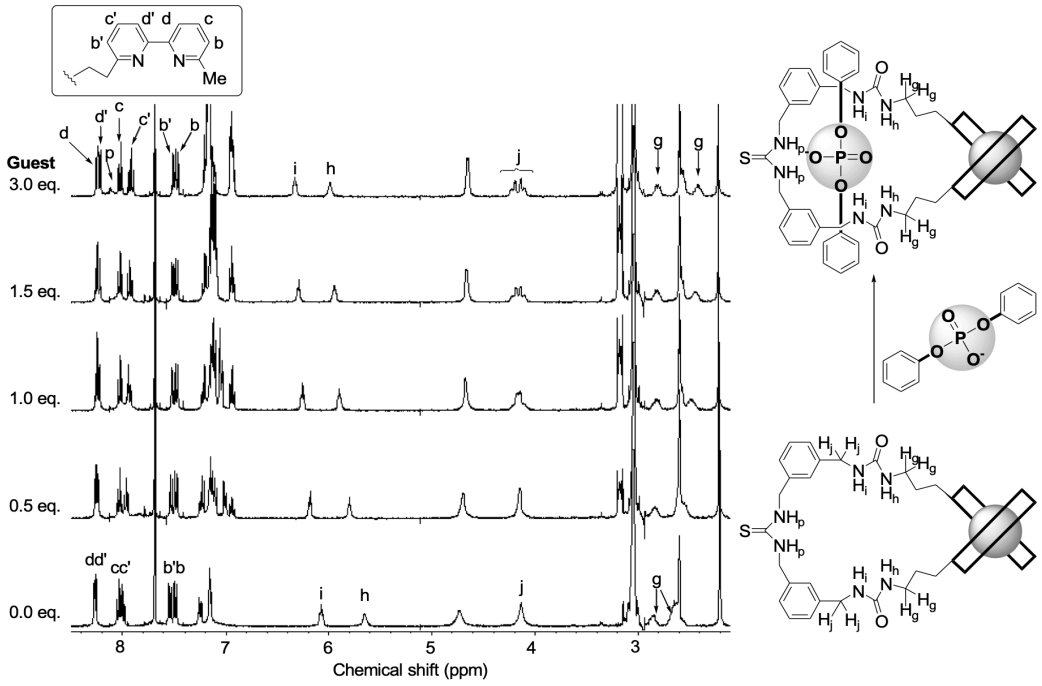

Figure S25. A titration experiment of [**1**·Cu]PF_6 and nBu$_4$N[(PhO)$_2$P(O)O] (^{1}H NMR, $CDCl_3$/CD_3CN/DMSO-d_6 = 15/1/4, 400 MHz, [**1**·Cu] = 2.0 mM).

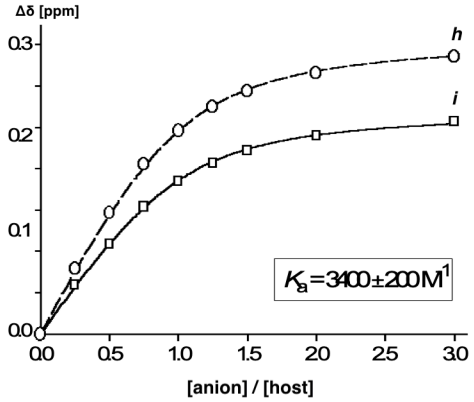

Figure S26. A least squares fitting to determine the binding constant K_a of $(PhO)_2P(O)O^-$ and [**1**·Cu]$^+$ (data of NMR signals of urea ^{1}H(*h* and *i*)).

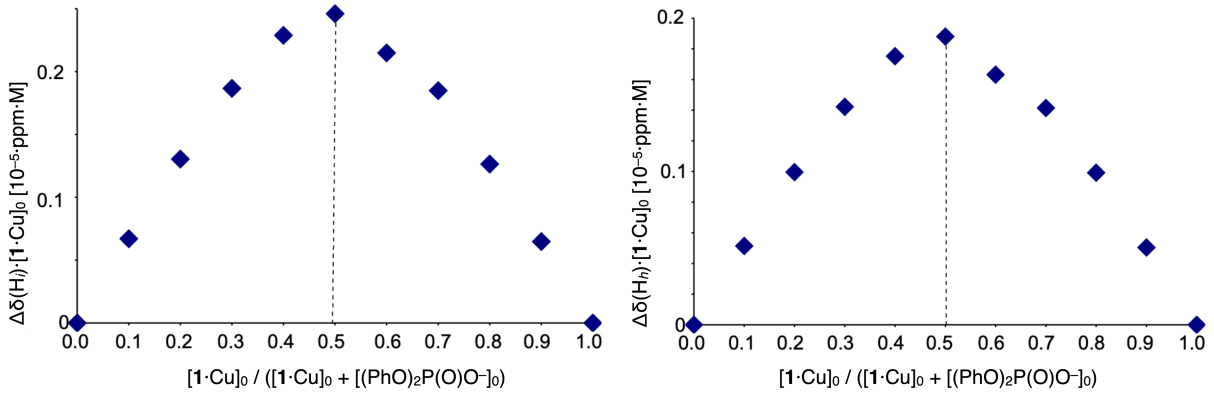

Figure S27. Job plots to determine the binding stoichiometry of $(PhO)_2P(O)O^-$ and [**1**·Cu]$^+$ (^{1}H NMR, $CDCl_3$/CD_3CN/DMSO-d_6 = 15/1/4, 400 MHz, [**1**·Cu]$_0$ + [$(PhO)_2P(O)O^-$]$_0$ = 4.0 mM, data of NMR signals of urea ^{1}H(*h* and *i*)).

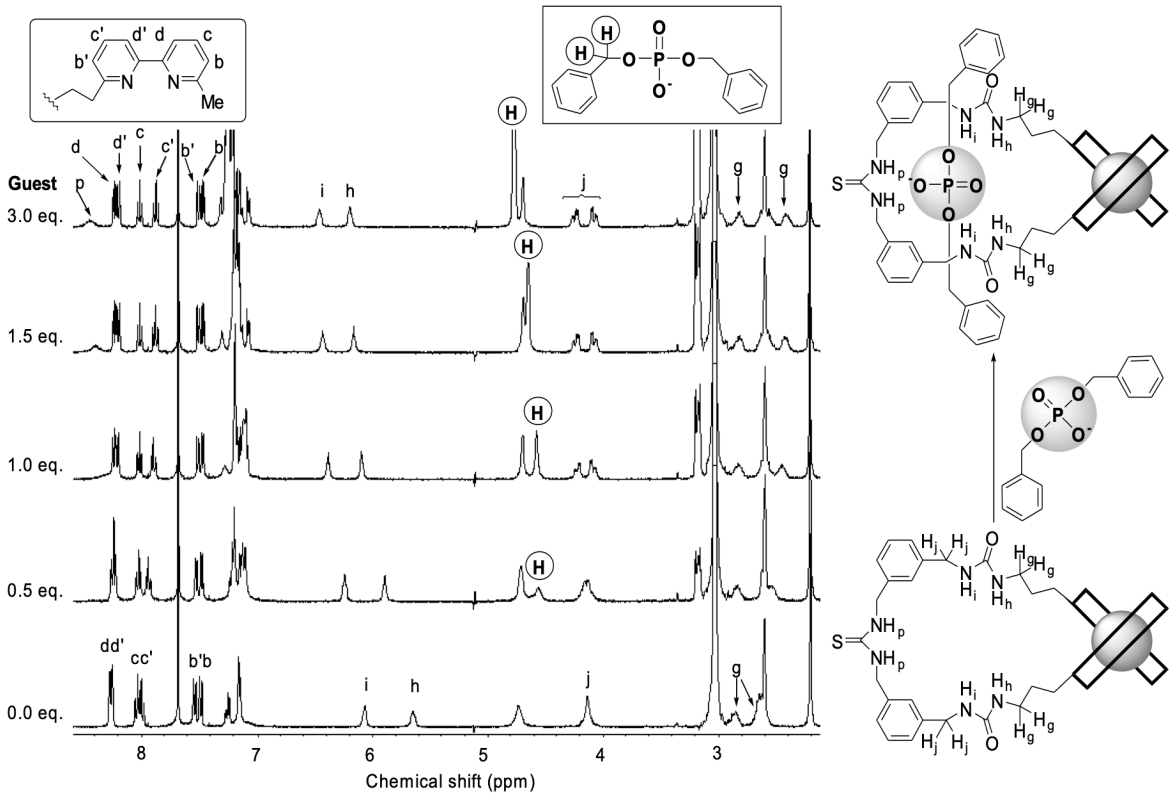

Figure S28. A titration experiment of [**1**·Cu]PF_6 and nBu$_4$N[(BnO)$_2$P(O)O] (^{1}H NMR, $CDCl_3$/CD_3CN/DMSO-d_6 = 15/1/4, 400 MHz, [**1**·Cu] = 2.0 mM).

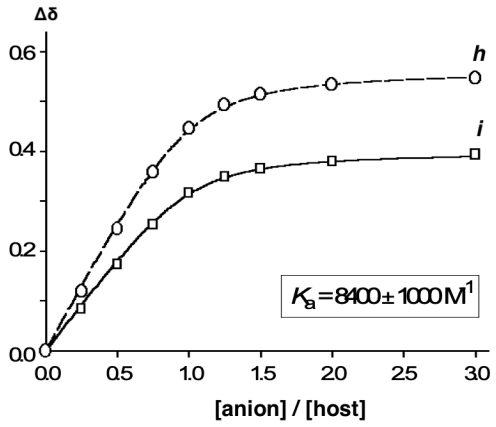

Figure S29. A least squares fitting to determine the binding constant K_a of (BnO)$_2$P(O)O$^-$ and [**1**·Cu]$^+$ (data of NMR signals of urea ^{1}H(*h* and *i*)).

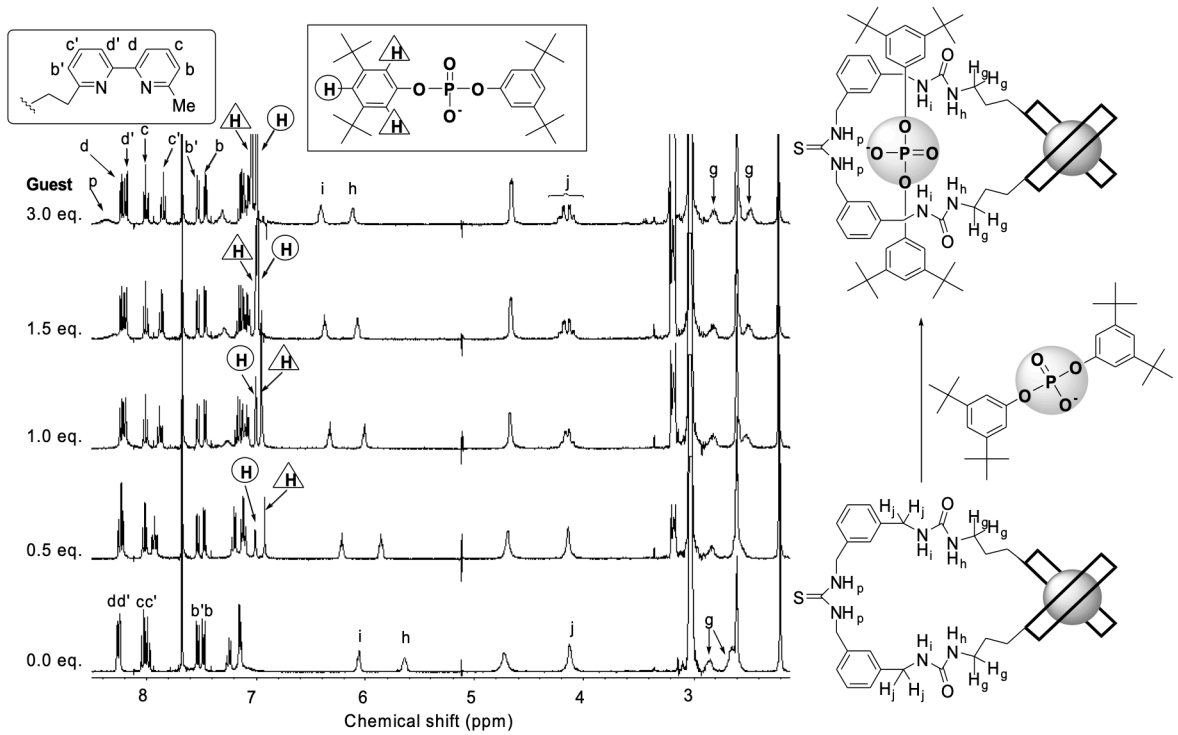

Figure S30. A titration experiment of [**1**·Cu]PF_6 and nBu$_4$N[(3,5-di-tBu$C_6H_3O)_2$P(O)O] (^{1}H NMR, $CDCl_3$/CD_3CN/DMSO-d_6 = 15/1/4, 400 MHz, [**1**·Cu] = 2.0 mM).

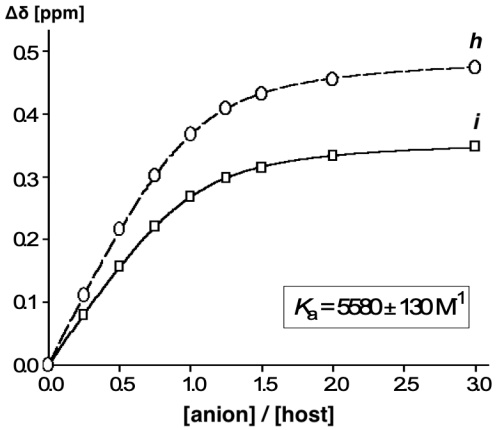

Figure S31. A least squares fitting to determine the binding constant K_a of (3,5-di-tBu$C_6H_3O)_2$P(O)O$^-$ and [**1**·Cu]$^+$ (data of NMR signals of urea ^{1}H(*h* and *i*)).

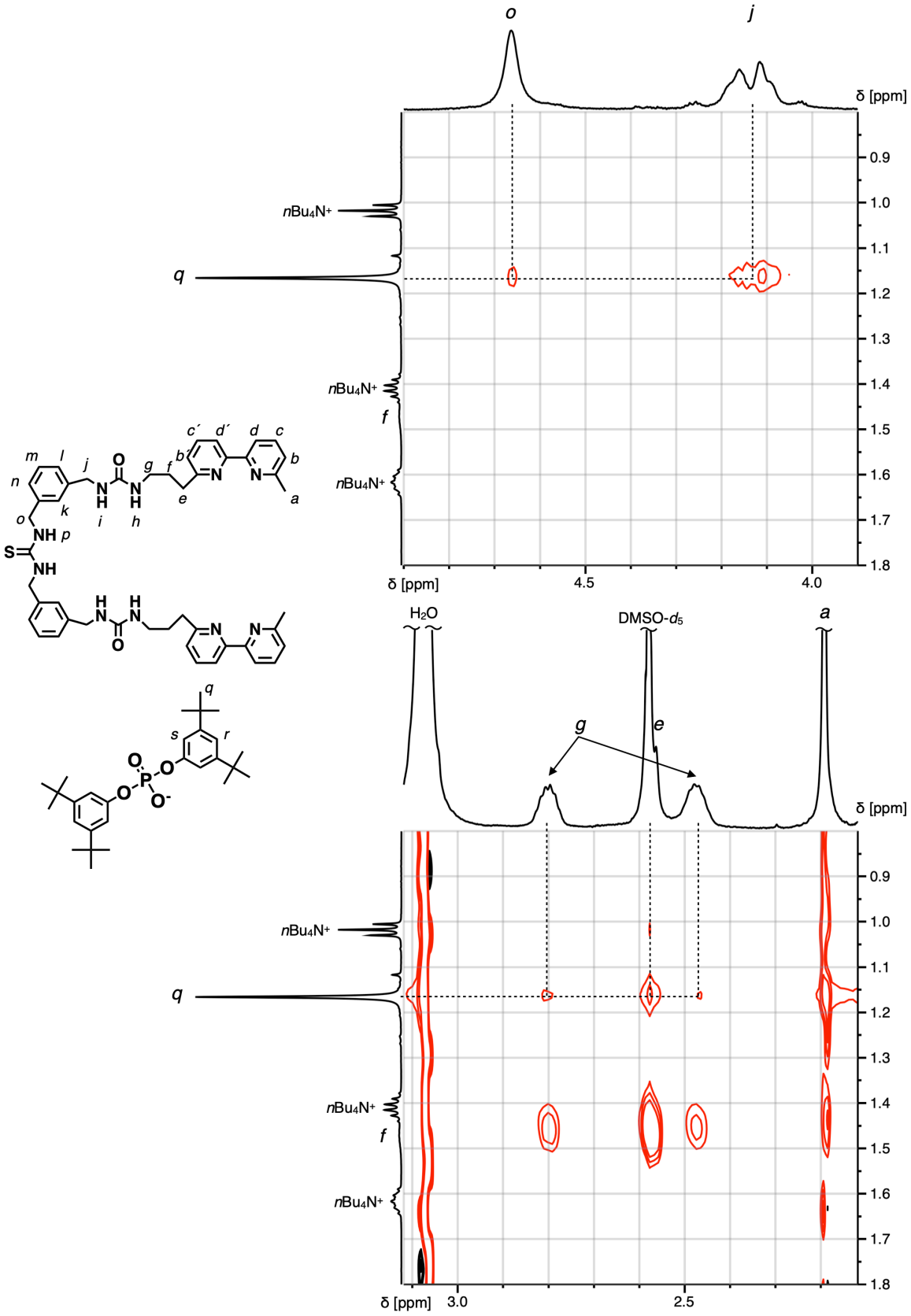

Figure S32. ^{1}H–^{1}H ROESY spectra of rotaxane ([**1**·Cu]PF_6 + *n*Bu_4N[(3,5-di-*t*$BuC_6H_3O)_2P(O)O$] (1 equiv.) (600 MHz, $CDCl_3$/CD_3CN/DMSO-d_6 = 15/1/4).

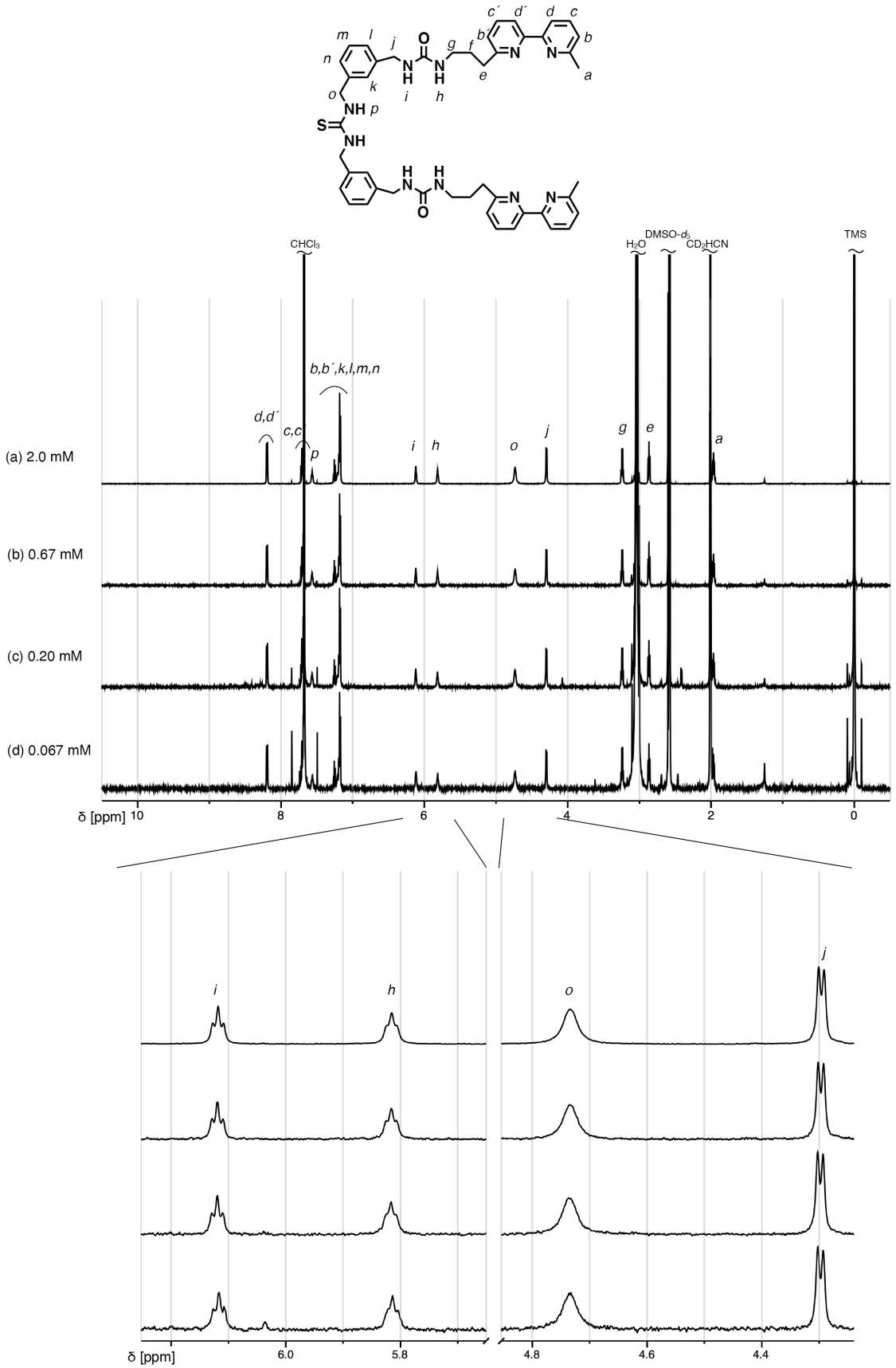

Figure S33. ^{1}H NMR spectra of ligand **1** at different concentrations (600 MHz, $CDCl_3/CD_3CN$/DMSO-d_6 = 15/1/4). The intensities of the spectra are normalized. (a) 2.0 mM (16 scans). (b) 0.67 mM (16 scans). (c) 0.20 mM (128 scans). (d) 0.067 mM (512 scans).

References for the Supporting Information

S1. M. Khoukhi, M. Vaultier and R. Carrié, *Tetrahedron Lett.*, 1986, **27**, 1031–1034.

S2. R. Gross, G. Dürner and M. W. Göbel, *Liebigs. Ann. Chem.*, 1994, 49–58.